American Mineralogist, Volume 86, pages 731–739, 2001

Mössbauer and XAS study of a green rust mineral; the partial substitution of Fe^{2+} by Mg^{2+}

P. REFAIT,[1,*] M. ABDELMOULA,[1] F. TROLARD,[2] J.-M. R. GÉNIN,[1] J.J. EHRHARDT,[1] AND G. BOURRIÉ[2]

[1]Laboratoire de Chimie Physique et Microbiologie pour l'Environnement, UMR 7564 CNRS-Université Henri Poincaré, F-54600 Villers-lès-Nancy, France

[2]INRA-Géochimie des Sols et des Eaux, CEREGE, BP80, F-13545 Aix-en-Provence Cedex 4, France

ABSTRACT

Layered double hydroxysalt green rusts, GRs, are very reactive compounds and their general formula, $[Fe^{2+}_{(1-x)}\ Fe^{3+}_{x}\ (OH)_2]^{x+}\ [\ x/n\ A^{n-}\cdot m\ H_2O]^{x-}$, where x is the ratio Fe^{3+}/Fe_{tot}, reflects the structure in which brucite-like layers alternate with interlayers of anions A^{n-} and water molecules. A GR mineral was extracted from hydromorphic soils in Fougères (France) and studied by X-ray absorption spectroscopy (XAS) and transmission Mössbauer spectroscopy (TMS). The XAS spectrum at the Fe *K* absorption edge of this mineral proved to be very similar to that of synthetic GRs. However, the radial distribution function obtained for the GR mineral proved to be intermediate between those of $GR(CO_3^{2-})$ and pyroaurite, that is between the Fe^{2+}-Fe^{3+} and Mg^{2+}-Fe^{3+} hydroxycarbonates. Consequently, a partial substitution of Fe^{2+} by Mg^{2+} occurs, leading to the general formula of $[Fe^{2+}_{(1-x)}Mg^{2+}_{y}Fe^{3+}_{x}(OH)_{(2+2y)}]^{x+}\ [x/n\ A^{n-}\cdot m\ H_2O]^{x-}$ where A^{n-} is the interlayer anion. Unfortunately, the XAS spectra of various GR proved to be independent of the interlayer anion, and the nature of the anions present in the mineral GR could not be determined. The Mössbauer spectrum of the mineral, measured at 77 K, is composed of four quadrupole doublets: D_1 and D_2 due to Fe^{2+} [$\delta \cong 1.26$ mm/s and $\Delta E_Q \cong 2.5$ and 2.9 mm/s, respectively] and D_3 and D_4 due to Fe^{3+} [$\delta \cong 0.46$ mm/s and $\Delta E_Q \cong 0.5$ and 1.0 mm/s, respectively]. Finally, synthetic Mg^{2+}-Fe^{2+}-Fe^{3+} hydroxycarbonates could be prepared by coprecipitation from Mg and Fe salts and lead to Mössbauer spectra similar to that of the mineral. In particular, the partial substitution of Fe^{2+} by Mg^{2+} proved to be consistent with the existence of the unusual doublet D_4.

INTRODUCTION

The mobility of Fe is of utmost importance in soil- and ore-forming, biogeochemical and environmental processes because of its abundance and its variety of oxidation states. In oxidizing conditions, Fe oxides present are goethite and hematite. The relative stability of these latter minerals is affected first by water activity, secondly by particle size (Ferrier 1966), and thirdly by Al^{3+} substitutions in the lattice (Trolard and Tardy 1987). In moderately reducing conditions, Fe is reduced and siderite occurs in sediments, whereas in strongly reducing conditions, sulfate is reduced, too, and pyrite forms. The relative stabilities of hematite, siderite, and pyrite have been discussed using E_h-pH diagrams by Krumbein and Garrels (1952), Huber and Garrels (1953), Garrels and Christ (1965). In the system air + ocean + sediments, Sillén (1967) considered FeOOH, Fe_3O_4, FeS_2 and FeS to be successively stable, from oxidizing to strongly reducing conditions. Hydromorphic soils characterized by moderately reducing conditions were recognized very early (Vysotskii 1905) as showing a distinct greenish-blue chroma that upon exposure to the air turned yellowish, and ascribed to the fact that some Fe was undoubtedly present as FeO. This green-blue color was much later suggested by Taylor (1981) to come from Fe^{2+}-Fe^{3+} double layered hydroxides, commonly named green rusts (GRs) i.e., Fe^{2+}-Fe^{3+} hydroxy-chlorides and -sulfates or -carbonates. The solid phases that control iron in soil solution have long been searched for, but no equilibrium between Fe^{3+} oxides and solution was observed in moderately reducing conditions and instead evidence for the equilibrium with a mixed Fe^{2+}-Fe^{3+} hydroxide was derived from laboratory experiments (Arden 1950) or field soil solution studies (Ponnamperuma et al. 1967; Ponnamperuma 1972; Lindsay 1979). These phases were designated as "the theoretical compound hydromagnetite, $Fe_3(OH)_8$" and considered as metastable phases with no explicit link being made between this compound and GRs (Taylor 1981). It was only recently that such a mineral, for which the name fougerite was proposed, was characterised by Mössbauer and Raman spectroscopies in hydromorphic soils (Trolard et al. 1996, 1997). It was assumed to be one of the various forms of GRs. By analogy with pyroaurite, it consists of positively charged brucite-like layers

*Present adress: Laboratoire d'Etudes des Matériaux en Milieux Agressifs, Université de La Rochelle, Avenue Michel Crépeau, F-17042 La Rochelle Cedex 1, France. E-mail: prefait@univ-lr.fr

of $[Fe^{2+}_{(1-x)}\ Fe^{3+}_{x}\ (OH)_2]^{x+}$ alternating with negatively charged interlayers made of anions A^{n-} and water molecules $[x/n\ A^{n-} \cdot (1-x)\ H_2O]^{x-}$. The equilibrium conditions observed between soil solution and minerals suggested that the interlayer anions could be OH^-, leading to the compact dehydrated formula $Fe(OH)_{(2+x)}$. It was shown that x ranges 1/3 to 2/3 using the Fe^{3+}/Fe_{tot} ratio measured by Mössbauer spectroscopy (Génin et al. 1998). The value $x = 2/3$ coincides with $Fe_3(OH)_8$. It was then proved, from analysis of soil solutions and solids from the same field sites, that $Fe(OH)_{(2+x)}$ does govern the iron solubility in soil solution and groundwater (Troard et al. 1997; Génin et al. 1998; Bourrié et al. 1999).

Because this mineral is strongly suspected to be associated with bacterial activity on ferric minerals in anoxic waterlogged soils (Génin et al. 1998), its potential for reducing pollutants has been stressed (Génin et al. 2001). This assumption was strengthened by several studies demonstrating that a synthetic GR, the sulfated one, was able to reduce in abiotic conditions some major polluting species such as nitrate into ammonium (Hansen et al. 1996), selenate into Se(0) (Myneni et al. 1997; Refait et al. 2000) or chromate into Cr^{3+} (Loyaux-Lawniczak et al. 1999; 2000). A mineral that displays structural features similar to those of a Fe^{2+}-Fe^{3+} double-layered hydroxide and is obtained by bacterial activity in soils at the depth of the water table could play a major role in the coupling of biogeochemical cycles. A better characterization of the occurrence, chemical composition, structure and reactivity of the mineral is thus of great interest to define soil and water management practices.

Unfortunately, because this mineral is scattered in soils, dilute (total Fe content in the soil is about 2–3.9%) and very labile, X-ray diffraction (XRD), which is not selective, is inappropriate for determining its structure. Using X-ray absorption spectroscopy (XAS), one gets information involving only the Fe-containing compounds by investigating the Fe K absorption edge. XAS can yield structural information, because it probes the local environment of Fe atoms, and X-ray absorption near edge structure (XANES) can provide the oxidation states. The similarity between the XAS spectrum of the mineral and that of synthetic GRs is one more reason to define it as a "GR mineral". However, it demonstrates that Mg^{2+} ions substitute for some Fe^{2+} ions. The second part is thus devoted to the preparation and study of Mg^{2+}-Fe^{2+}-Fe^{3+} double layered hydroxides, using carbonate as the interlayer anion.

Experimental methods

Synthetic sample preparation

Three reference compounds were prepared for the EXAFS study, GR(Cl^-) the Fe^{2+}-Fe^{3+} hydroxychloride, GR(CO_3^{2-}) the Fe^{2+}-Fe^{3+} hydroxycarbonate, and pyroaurite (Mg^{2+}-Fe^{3+} hydroxycarbonate). The GR(CO_3^{2-}) sample was prepared according to the method developed previously by Drissi et al. (1994, 1995). Ferrous hydroxide was precipitated from 0.18 M $FeSO_4 \cdot 7H_2O$ and 0.3 M NaOH solutions and a 0.18 M Na_2CO_3 solution was added as a source of carbonate ions. All reagents were provided by PROLABO and had a maximum impurity content of 2%. The suspension was then aerated at the interface between solution and laboratory atmosphere with a magnetic stirring (500 rpm) ensuring a progressive homogeneous oxidation of the $Fe(OH)_2$ precipitate into GR(CO_3^{2-}). A thermostat maintained the temperature at 25 ± 0.5 C. The reaction was monitored by recording the redox potential of the solution, by use of a Pt electrode and a saturated calomel electrode as reference. At the end of the formation of the GR, the suspension was quickly poured into a sealed flask to shelter it from air. GR(Cl^-) was prepared in a similar way, by precipitation and oxidation of a $Fe(OH)_2$ aqueous suspension, following the procedure of previous studies (e.g., Refait et al. 1998b). The reagents were $FeCl_2 \cdot 4H_2O$ (0.24 M) and NaOH (0.4 M).

Synthetic pyroaurite samples can also be prepared using this procedure (Refait et al. 1998d). In this case, a Mg^{2+}-Fe^{2+} hydroxide was precipitated by mixing solutions of Fe^{2+} and Mg^{2+} sulfates ($FeSO_4 \cdot 7H_2O$ and $MgSO_4$) with caustic soda. The concentrations were set at [Mg] + [Fe] = 0.18 M, with Mg/Fe = 2.5, [NaOH] = 0.3 M and $[Na_2CO_3]$ = 0.18 M. The product was obtained at the end of the overall oxidation process, where no Fe^{2+} cations remained. Its composition was then about $Mg_5Fe_2(OH)_{14}CO_3 \cdot nH_2O$.

Samples of Mg^{2+}-Fe^{2+}-Fe^{3+} hydroxycarbonate were prepared in a totally different way, by precipitation from Mg and Fe salts, NaOH and Na_2CO_3 solutions, a process much more realistic for the formation of such minerals in nature than the oxidation of $(Mg,Fe)(OH)_2$ hydroxides. Due to the affinity of such hydroxy-compounds for carbonate anions, the presence of other anions, e.g., SO_4^{2-} or Cl^-, provided by the metal salts, does not lead to the formation of the corresponding compounds (Miyata 1983; Mendiboure and Schöllhorn 1986; Refait et al. 1997). In the first case, a 0.06 M $MgSO_4$ + 0.06 M $Fe^{2+}SO_4 \cdot 7H_2O$ + 0.06 M $Fe^{3+}Cl_3 \cdot 6H_2O$ solution was added to a 0.3 M NaOH + 0.18 M Na_2CO_3 solution; cations concentrations were chosen so that the ratios Fe/Mg and $[Mg^{2+} + Fe^{2+}]/Fe^{3+}$ were both equal to 2. In contrast, a 0.045 M $MgSO_4$ + 0.09 M $Fe^{2+}SO_4 \cdot 7H_2O$ + 0.045 M $Fe^{3+}Cl_3 \cdot 6H_2O$ solution was added to a 0.3 M NaOH + 0.18 M Na_2CO_3 solution in the second case, implying that Fe/Mg and $[Mg^{2+} + Fe^{2+}]/Fe^{3+}$ are equal to 3. Both samples were aged 24 hours in a sealed flask before analyses.

Mineral sampling

Reductomorphic soils display, in some subsurface horizons, a green-blue color, characteristic of "gley" horizons (Vysostski 1905). A profile described by Trolard et al. (1997) and Bourrié et al. (1999) was selected in the forest of Fougères (Brittany). A sample was extracted in the field, at a depth of 90 cm. At that locality, the soil profile displays two major units: a histic horizon down to 15 cm and a granitic saprolite down to 120 cm followed by an oxidized horizon with accumulation of Fe^{3+} oxides. The waterlogged soil is located near a spring. A large field sample (approx. 1.25 dm^3) including the soil solution was extracted and placed in a sealed container. The 10 mg samples to be analyzed by XAS or transmission Mössbauer spectroscopy (TMS) were taken out of the core of the oversized field sample and prepared in the laboratory under a nitrogen atmosphere to avoid oxidation.

Analysis

Synthetic [Mg^{2+}-Fe^{2+}]-Fe^{3+} GR samples were analyzed by powder X-ray diffraction (PXRD) and transmission Mössbauer spectroscopy (TMS) at 77 ± 1 K. Because the GR mineral is diffuse, scattered and mixed with other compounds, PXRD could not be used for its characterization and thus only TMS results will be presented. PXRD patterns were obtained with a classical powder diffractometer (Philips) using the Co$K\alpha$1 wavelength (λ = 0.17889 nm). Mössbauer spectra were accumulated at 77 K with a constant-acceleration spectrometer and a 512 multichannel analyzer, manufactured by Halder Elektronic GMBH, and a 50 mCi source of ^{57}Co in Rh maintained at room temperature. The velocity was calibrated with a 25 m foil of α-Fe at room temperature and the isomer shifts will thus be given with respect to this reference. Precautions were taken to avoid spurious oxidation before and during analysis. Thus, in any case, the samples were first filtered on a paper under an inert atmosphere, in a nitrogen-purged Jacomex controlled atmosphere glove box. For XRD measurements, they were deposited on a glass platelet and coated with glycerol to limit the oxidizing action of air (Hansen 1989). For TMS measurements, they were set in the sample holder and introduced in the cryostat (Cryo Industries of America) and then sheltered from the action of O_2. The amount of materials being optimized (10 mg of Fe per cm^2), the spectra can be reasonably approximated by a sum of lines with Lorentzian shape (thin-absorber approximation). This proved to be appropriate in the case of GRs because the peaks have a perfectly Lorentzian shape with small widths of about 0.3 mm/s (see Refait et al. 1998b, 1999 for example). A set of free parameters are then altered in such a way that a goodness-of-fit criterion, the minimal chi-square (χ^2), is optimized. The free parameters are those which are only mutually bounded via the χ^2 minimization procedure. For quadrupole doublets, these parameters are the isomer shift δ, the quadrupole splitting ΔE_Q, the half widths at half maximum Γ and the heights of the peaks RA, constrained to be equal for both lines of the doublet. The error on the determination of these parameters was estimated by analyzing three samples of the product and lead in most cases to an interval of ±0.02 mm/s.

The synthetic pyroaurite sample to be used as reference for the XAS study was previously checked by PXRD and TMS (15 ± 1 K) analyses. The PXRD pattern (Fig. 1) is typical of the $R\bar{3}m$ structure of pyroaurite and the lattice parameters a = 0.3090 ± 0.0005 nm and c = 2.313 ± 0.005 nm determined from the measured d_{hkl} data are in agreement with those generally accepted, that is a = 0.3109 and c = 2.341 nm (Allmann 1968). The TMS spectrum at 15 K is comprised of two quadrupole doublets D_0 and D_1. The main doublet D_0, representing 86 (±2)% of the total area, has hyperfine parameters typical of Fe^{3+} in octahedral sites, with δ = 0.49 ± 0.02 mm/s and ΔE_Q = 0.62 ± 0.02 mm/s. The second doublet D_1, computer-fitted with δ = 0.43 ± 0.02 mm/s and ΔE_Q = 0.20 ± 0.04 mm/s rather resembles to a single peak and may correspond to an asymmetry of D_0. This effect is due to preferred orientation of the crystals, a phenomenon commonly observed for such compounds (Koch 1998). Anyhow, those spectral components correspond to what is usually found for Fe^{3+} in such hydroxy-compounds (Refait et al. 1998a, 1998d). No other contributions are seen, implying

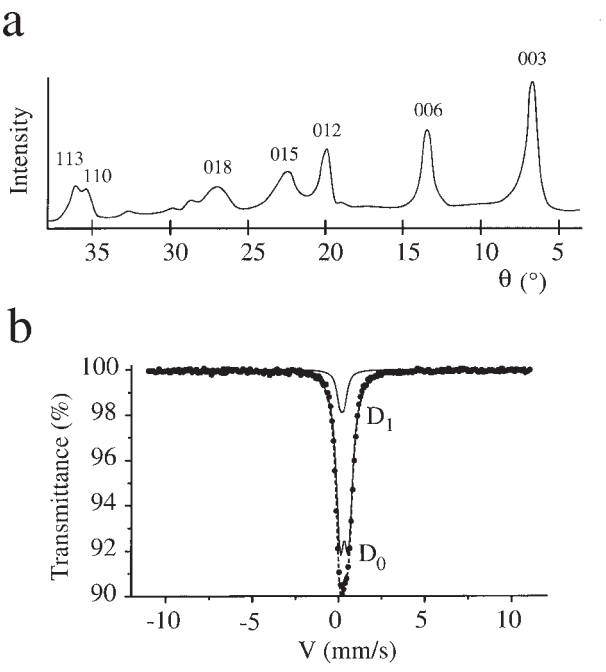

FIGURE 1. Powder XRD pattern (**a**) and Mössbauer spectrum measured at 15 K (**b**) of synthetic pyroaurite. XRD = Miller indices are expressed in the hexagonal representation of the $R\bar{3}m$ lattice; note that diffraction angle is θ. Mössbauer spectrum: dotted line = experimental curve; dashed line = global computed curve; solid line = components of the spectra.

that all of the Fe atoms in the sample are associated with the hydroxycarbonate.

XAS data were collected at the Fe K edge (7112 eV) at the D44 station of the DCI high energy ring (1.8 GeV, λ_c = 3.5 keV) of LURE (Orsay, France). Transmission mode measurements were carried out at about 77 K using a liquid nitrogen cryostat. Energy selection was made using a Si(311) double crystal monochromator which was detuned to reduce unwanted harmonics. Absorption was detected using He/Ne/air filled ion chambers. Samples were diluted with cellulose and pressed into pellets of 5 × 13 mm^2 in size. Preparation of the GRs samples and mineral was performed in a glove box under an inert gas (Ar) atmosphere to prevent oxidation.

At least four acquisitions were recorded for each sample and averaged before extraction of the extended X-ray absorption fine structure (EXAFS) signal. The WinXAS 97 program by Ressler (1997) was used for the data analysis. The pre-edge was removed by linear simulation and the atomic contribution after the edge was extracted by a 5th degree polynomial. The E_0 value was chosen at the first inflection point in the Fe absorption edge; k^3 weighted Fourier transforms of the EXAFS spectra were calculated between k_{min} ~ 2.5 and k_{max} ~ 13.5/$Å^{-1}$ using a Kaiser window with a τ parameter equal to 3.

The X-ray absorption near edge structure (XANES) parts were acquired from –150 to +190 eV with respect to the Fe K edge (7112 eV). The spectrum of EuPd was collected simultaneously with each data set for energy calibration, with the first

inflection of the Eu L_3 absorption edge taken to be 6977 eV. The incident X-ray energy was incremented by 0.5 eV intervals over the critical ranges of 6970 to 7000 eV (Eu L_3 edge) and 7100 to 7300 eV (Fe *K* edge) and by larger intervals of 3.0 eV elsewhere to reduce data collection times. The counting time was 1 second per point. Background subtraction and normalization were carried out using the winXAS 97 program (Ressler 1997).

RESULTS

XAS study of the mineral

The XANES part of the mineral spectrum (Fig. 2) contains information about the oxidation state and the local symmetry of the absorber (Stohr 1986; Bianconi 1980; Citrin 1986; Tadjeddine 1994). More precisely, the energy position of the absorption edge is dependent on the effective charge density of the absorber and reflects the tendency of an electron-deficient atom to bind more tightly the remaining electrons. Thus, the Fe^{3+} edge of goethite is shifted by 5 eV to higher energy in comparison to the Fe^{2+} edge of $FeCl_2$. The curves of GR(CO_3^{2-}) and of the GR mineral are similar, for the most part coalesced, and differences can only be seen at the top of the peak edge. The edge position is in both cases intermediate between that of $FeCl_2$ and that of FeOOH, and clearly demonstrates the presence of both Fe^{2+} and Fe^{3+} valence states. A look at the pre-edge peak region (Fig. 2b) confirms it. The $FeCl_2$ and FeOOH curves present one net peak, that of goethite shifted by 3–4 eV from that of $FeCl_2$, whereas the curves of the GRs present contributions from both Fe^{2+} and Fe^{3+}.

The PRDF of the mineral and those of synthetic GRs (Fig. 3) display the same set of peaks (P_1–P_6) and are found in agreement with previous studies on similar compounds (Roussel et al. 2000). Because of phase shifts, the observed distances differ from the real inter-atomic distances of about 0.04–0.045 nm. The first peak, P_1, is related to the octahedron of OH^- ions which surrounds the iron atom; the corresponding bond distance is about 0.2 nm. The next peak, P_2, is found at the Fe-Fe distance which corresponds to the parameter *a* of the $R\bar{3}m$ lattice, at about 0.31–0.32 nm. Roussel et al. (2000) demonstrated that the other smaller peaks, P_3-P_6, correspond to the hexagonal array of cations that is to the second, third, etc... Fe neighbors, because they are found in the sequence: $a\sqrt{3}$, $2a$, $a\sqrt{7}$, $3a$, as illustrated in Figure 4. The intensities of the peaks P_4 and P_6 are increased by the so-called focusing effect (Teo 1986; Lee and Pendry 1975) and superfocusing effect (Kuzmin and Parent 1994). These effects correspond to multiple scattering phe-

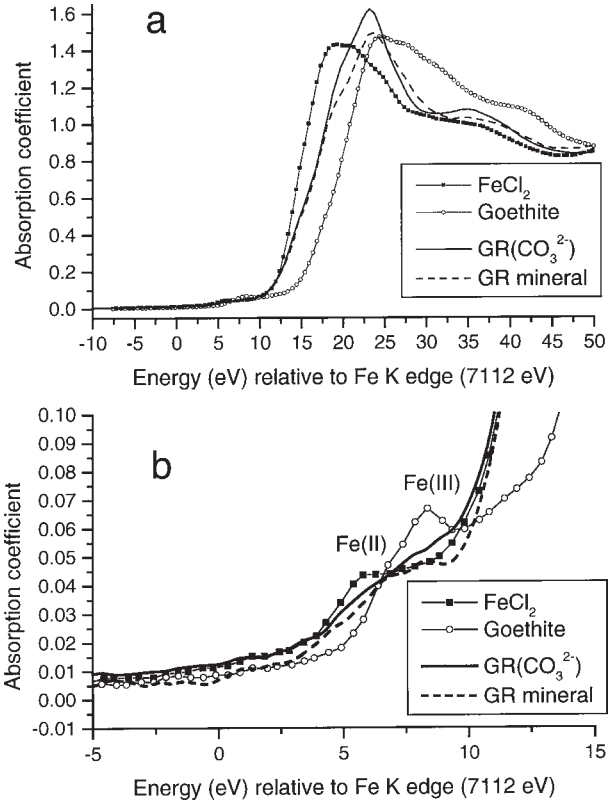

FIGURE 2. (**a**) Fe-K edge XANES spectra of synthetic GR(CO_3^{2-}) and GR mineral "fougerite" compared to those of reference compounds, $FeCl_2$ and goethite. Part **b** is the same as part **a** but with expanded scale and focused on the pre-edge peak region.

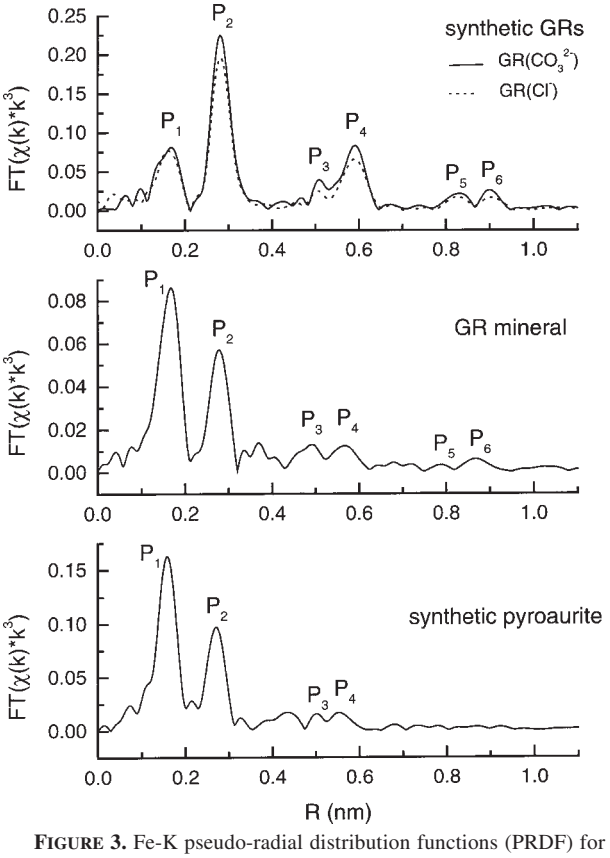

FIGURE 3. Fe-K pseudo-radial distribution functions (PRDF) for synthetic GRs [GR(CO_3^{2-}) and GR(Cl^-)], GR mineral "fougerite" and synthetic pyroaurite. PRDF are not corrected for phase shift functions. The real interatomic distances can be found approximately by adding about 0.04 nm to the distances given here.

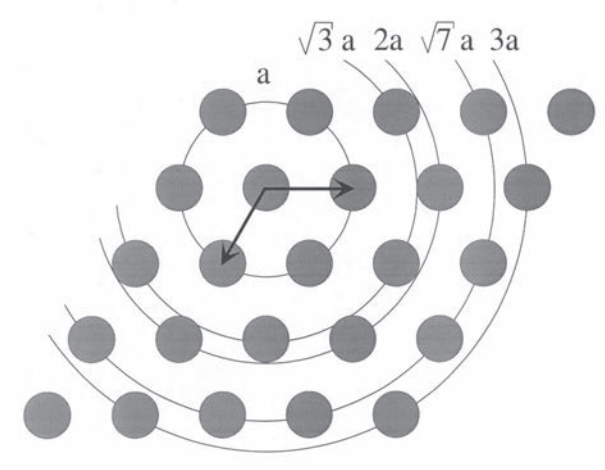

FIGURE 4. Portion of a hydroxide sheet showing the Fe-Fe distances in GRs.

nomena between 3 and 4 cations in collinear arrangement, respectively, and reflect the organisation of the cations.

None of the PRDF peaks can be attributed to back-scattering on atoms present in the interlayers. These species, anions or water molecules, are already far from the Fe ions, screened by the OH^- ions of the octahedra. This is demonstrated by the fact that GR(CO_3^{2-}) and GR(Cl^-) display the same PRDF. The slight differences observed in Figure 3 may arise from different *a* lattice parameters, because *a* = 0.316 nm for GR(CO_3^{2-}) (Drissi et al. 1995) whereas *a* = 0.319 nm for GR(Cl^-) (Refait et al. 1998b), but they remain within the experimental error. In contrast, the *c* parameters are significantly different, 2.25 nm in GR(CO_3^{2-}) and 2.4 nm in GR(Cl^-), due to the size of the interlayer anions, but this proves to have no influence on EXAFS spectra.

However, there exists a significant difference between the mineral and synthetic GRs. The Fe-Fe peak P_2 at distance *a* is much more intense in synthetic GRs than in the mineral sample. In order to understand the reason, the PRDFs of these three compounds must be compared to that of synthetic pyroaurite. It appears that the peaks corresponding to Fe-(Fe,Mg) distances, P_2-P_6, are drastically less intense than in synthetic GRs. According to Vucelic et al. (1997), there exists a local order so that Fe^{3+} cations never neighbor each other. In pyroaurite, the second shell can thus be considered as being composed of 6 Mg atoms. The PRDF of the mineral seems to be intermediate between that of GRs and that of pyroaurite, the small peaks P_3-P_6 being less attenuated than those of pyroaurite. This could have two origins: (1) Less iron is present, and one given Fe atom is surrounded by less than 6 Fe atoms or (2) Mg^{2+} cations are substituting for Fe^{2+} cations.

These assumptions were checked by examining the contribution to EXAFS of peak P_2. This contribution is obtained by back-Fourier transformation of the PRDF curve with a R window ranging from 0.259 to 0.364 nm. In the case of synthetic GRs, the back scattering atoms are Fe and in the case of synthetic pyroaurite they are Mg. The signal obtained from P_2 for the mineral can thus be fitted as a combination of the signal obtained from P_2 in GR(CO_3^{2-}) (Fe-Fe signal) and that obtained from P_2 in synthetic pyroaurite (Fe-Mg signal).

We fit the Fe-(Fe,Mg) contributions to EXAFS for the GR mineral in three different ways (Fig. 5). In each case the fit was performed with experimental phase shifts and amplitude functions derived from GR(CO_3^{2-}) (6 Fe at 0.316 nm) and synthetic pyroaurite (6 Mg at 0.311 nm) and the number of first neighbors was fixed at 6. This approach is realistic because it was demonstrated that multiple scattering was weak under about 0.4 nm (Roussel et al. 2000).

The first fit (Fig. 5a) was attempted with only a Fe-Fe signal. It proved impossible to fit correctly the signal of the mineral with a number of neighboring cations fixed at 6. To test the first assumption quoted above, i.e., less Fe is present, this number was left free. It decreased down to 1.5, for a reliability factor

$$R_f = \frac{\sum_{i=1}^{N} \left| y_{exp}(i) - y_{theo}(i) \right|}{\sum_{i=1}^{N} \left| y_{exp}(i) \right|}$$

equal to 16%. But such a number of neighboring cations is too

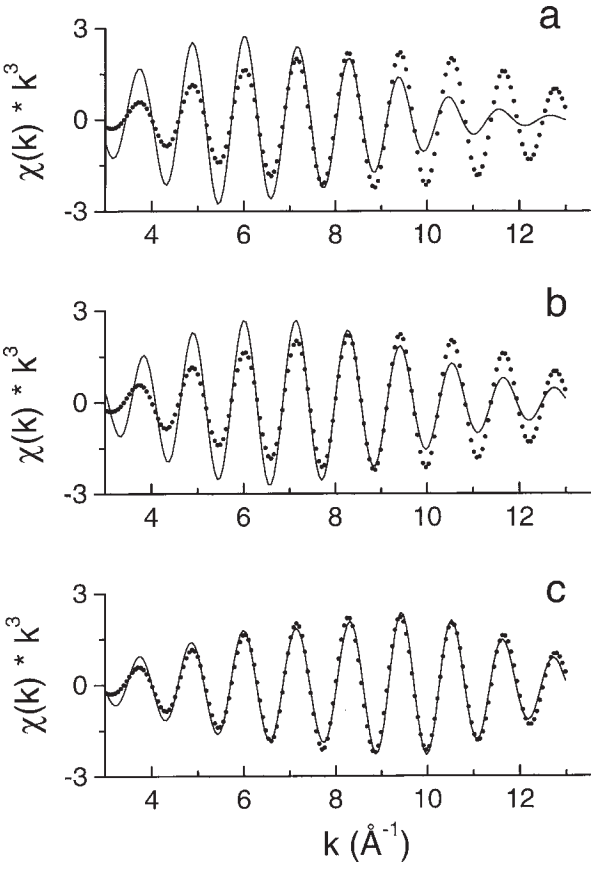

FIGURE 5. Fourier filtered Fe-(Fe,Mg) contributions to EXAFS for GR mineral "fougerite" fitted with (**a**) only Fe-Fe contribution, (**b**) only Fe-Mg contribution and, (**c**) Fe and Mg contributions. Dotted lines = experimental curve; solid line = fit.

small to be realistic and would suggest a totally different crystal structure for the mineral, which could not explain why the XAS and Mössbauer spectra of the mineral are similar to those of synthetic GRs. Thus this first assumption must be discarded. The second attempt (Fig. 5b) to fit the P_2 contribution to EXAFS only involved a Fe-Mg signal, and resulted in a similarly poor fit.

Finally, it proved rather satisfactory, even though the reliability factor remains at 19%, to fit the curve of the mineral with both Fe-Fe and Fe-Mg signals (Fig 5c). The corresponding parameters are in Table 1. This model resulted in similar Fe-Fe and Fe-Mg distances, giving an average *a* value of 0.3125 nm, intermediate between those found for GRs and that of pyroaurite. Parameter $\Delta\sigma$ measured the disorder with respect to the reference compounds. Because the spectra were collected at 77 K it can be assumed that the thermal vibrations of atoms are small, similar in the GR mineral and in the reference compounds. Then $\Delta\sigma$ measures essentially a variation of the static disorder that is of the distribution of the interatomic distances.

The average cation proportion obtained for the mineral is 1 Fe per 2 Mg. The error made on the number of backscatterers can be estimated at about 20–30%, thus the ratio Mg/Fe may be between 3 and 1. Moreover, it cannot be excluded that a partial ordering among Fe and Mg cations occurs. Therefore, the local proportion would differ from the overall one. Figure 6 shows an example. The hexagonal array of cations presented corresponds to an average Mg/Fe ratio of 1, but the ordering of Mg and Fe leads to a local value, that is the value viewed from a given Fe atom, of Mg/Fe = 2. For these various reasons it is not possible to quantify the proportion of Mg in the mineral.

TABLE 1. Structural parameters for Fe-(Fe,Mg) contributions in the GR mineral derived from EXAFS

Cation	*N*	*R* (nm)	$\Delta\sigma$ (nm)
Fe	2 (± 0.5)	0.312 (± 0.0005)	0.004 (±0.003)
Mg	4 (± 1)	0.313 (± 0.0005)	0.003 (±0.002)

Note: The *R* window was taken from 0.259 to 0.364 nm. ΔE_0, is the correction term to the absorption edge threshold, was determined to be 9 (±1) eV. *N* is the number of cations in the first shell, *R* is the Fe to cation distance and $\Delta\sigma$ is the difference of the Debye-Waller factor between the corresponding model compound, $GR(CO_3^{2-})$ for Fe-Fe and pyroaurite for Fe-Mg, and the sample.

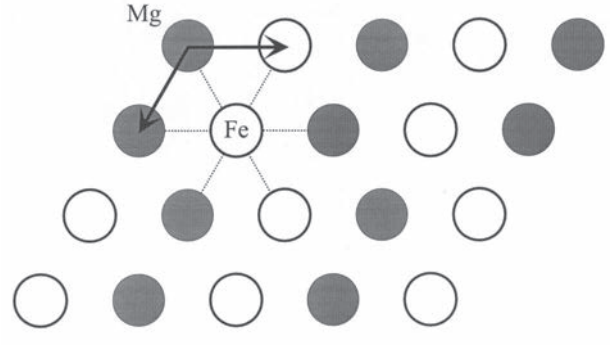

FIGURE 6. Hexagonal array of cations showing ordering of Fe and Mg for an overall ratio Mg/Fe = 1. Fe atoms are in white, Mg atoms in grey.

All that we can say is that Mg is a rather important component.

Synthetic Mg^{2+}-Fe^{2+}-Fe^{3+} hydroxycarbonates

Powder-XRD patterns of the two synthetic samples are similar to that presented in Figure 7. All the powder lines of a green rust compound with pyroaurite-like structure (Allmann 1968) are visible. No other lines are seen and the coprecipitation method of preparation gives rise to a single phase. Thus, in agreement with the quantities of reactants, the formulae of the samples would be $[Fe_4^{2+}Mg_2^{2+}Fe_2^{3+}(OH)_{16}]^{2+}\cdot[CO_3\cdot nH_2O]^{2-}$ and $[Fe_2^{2+}Mg_2^{2+}Fe_2^{3+}(OH)_{12}]^{2+}\cdot[CO_3\cdot nH_2O]^{2-}$. The lattice parameters of the samples, determined from the measured d_{hkl} data, are a = 0.3152 and 0.3126 ± 0.0005 nm and c = 2.3243 and 2.272 ± 0.004 nm, respectively. These values must be compared to those of $GR(CO_3^{2-})$ and pyroaurite, i.e., a = 0.316 and 0.311 nm and c = 2.245 and 2.341 nm, respectively (Allmann 1968; Drissi et al. 1995). Note also that the value a = 0.3126 nm measured for $[Fe_2^{2+}Mg_2^{2+}Fe_2^{3+}(OH)_{12}]^{2+}\cdot[CO_3\cdot nH_2O]^{2-}$ is that found by EXAFS for the mineral (Table 1).

Mössbauer spectra are presented in Figure 8 and compared to that of the mineral. Hyperfine parameters obtained from computer fitting with Lorentzian-shape lines are given in Table 2. The measured Fe^{3+}/Fe_{tot} ratios are close to those expected from the initial quantities of reactants, that is 41 vs. 33% expected and 56 vs. 50 % expected. The spectra had to be fitted with four quadrupole doublets. D_1 and D_2 correspond to Fe^{2+} ions whereas D_3 and D_4 correspond to Fe^{3+} ions. According to the crystal structure of GRs (Refait et al. 1998b), there would be one crystal site for Fe^{2+} and another one for Fe^{3+}. The Mössbauer spectrum of the compound $[Fe_2^{2+}Mg_2^{2+}Fe_2^{3+}(OH)_{12}]^{2+}\cdot[CO_3\cdot nH_2O]^{2-}$ was then fitted with only two doublets, namely D_1 for Fe^{2+} and D_3 for Fe^{3+} (Fig. 8a). This fit proved unsatisfactory, as indicated by the error curve (exp-theo), and regions of the spectra where contributions were lacking, indicated by arrows on the figure, appeared clearly. Moreover, the full widths at half maximum proved to be abnormally large, e.g., 0.56 mm/s for the peaks of D_3. Then doublet D_4 had to be added in order to obtain a satisfactory fit of the central zone, that is between 0 and 1 mm/s, and doublet D_2 proved necessary to take into account the asymmetry of the external peak at 2.5

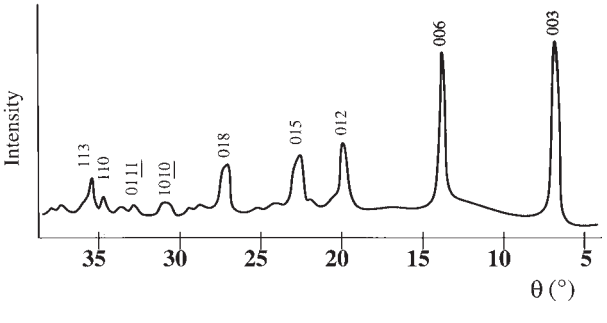

FIGURE 7. Powder XRD pattern of the synthetic green rusts where Fe^{2+} ions are partially substituted by Mg^{2+} ions. No other phase than a GR is observed. Miller indices are expressed in the hexagonal representation of the $R\bar{3}m$ lattice.

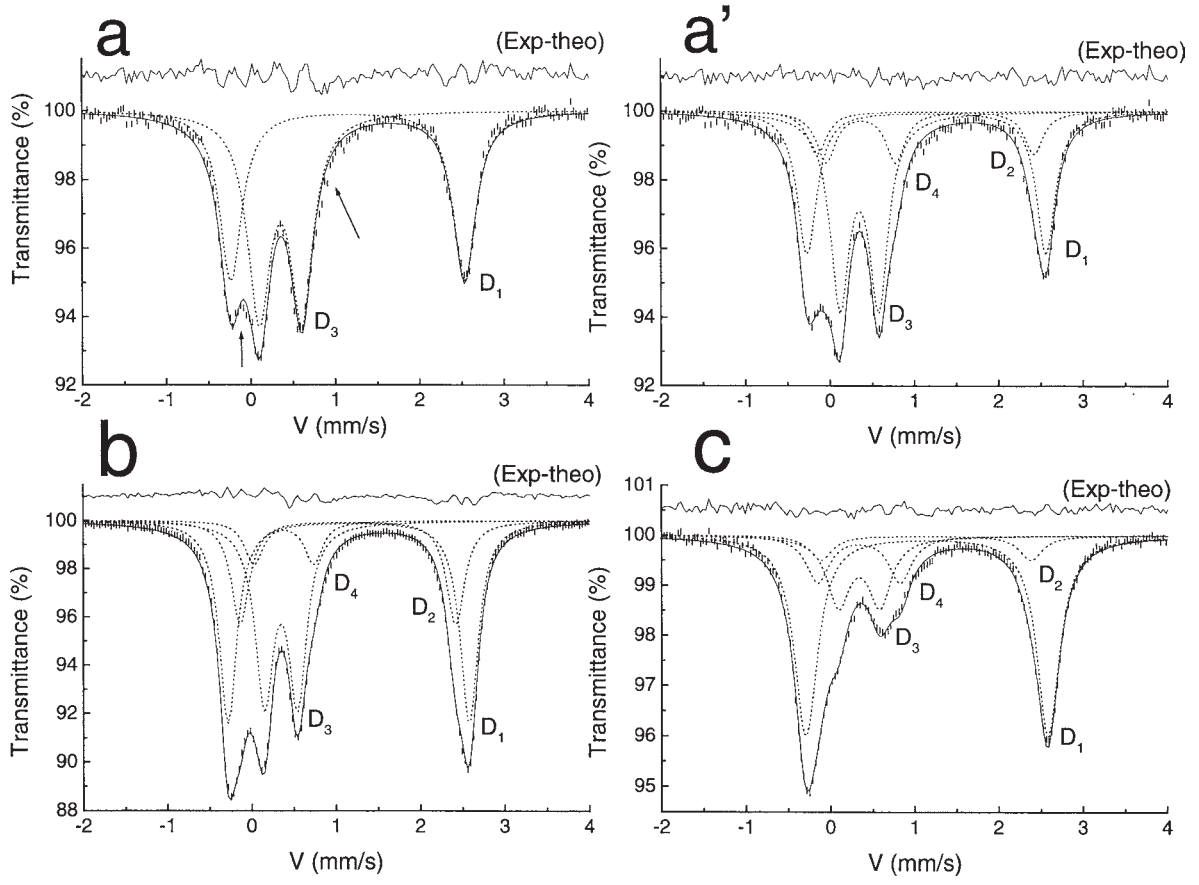

FIGURE 8. Mössbauer spectra measured at 77 K of two synthetic GRs obtained by coprecipitation of $[Mg^{2+}\text{-}Fe^{2+}][OH]_2$ suspensions in the presence of carbonate ions, compared with that of the mineral. (a) and (a'): Spectrum of $Fe_2^{2+}Mg_2^{2+}Fe_2^{3+}(OH)_{12}\,CO_3{\cdot}nH_2O$ fitted with two doublets (**a**) or four doublets (a'). (**b**) Spectrum of $Fe_4^{2+}Mg_2^{2+}Fe_2^{3+}(OH)_{16}\,CO_3{\cdot}nH_2O$ fitted with four doublets. (**c**) Spectrum of the GR mineral fitted with four doublets. Parallel lines = experimental curve; solid line = global computed curve. Dashed line = components of the spectra.

TABLE 2. Hyperfine parameters at 77 K of two synthetic samples of Mg^{2+}-Fe^{2+}-Fe^{3+} GR obtained by coprecipitation of Mg^{2+}, Fe^{2+}, and Fe^{3+} salt solutions in the presence of carbonate ions; the third sample is the GR mineral extracted in Fougères (Brittany, France)

	$[Fe^{2+}_{\frac{2}{3}}\,Mg^{2+}_{\frac{2}{3}}\,Fe^{3+}_{\frac{1}{3}}(OH)_{12}\,CO_3]$				$[Fe^{2+}_4\,Mg^{2+}_2\,Fe^{3+}_2(OH)_{16}\,CO_3]$				Mineral			
	δ	ΔE_Q	Γ	*RA*	δ	ΔE_Q	Γ	*RA*	δ	ΔE_Q	Γ	*RA*
D_1	1.27	2.83	0.26	31	1.27	2.85	0.25	39	1.27	2.86	0.32	59
D_2	1.25	2.58	0.26	13	1.27	2.54	0.25	20	1.25	2.48	0.32	07
D_3	0.47	0.44	0.26	42	0.47	0.39	0.25	33	0.46	0.48	0.32	20
D_4	0.49	0.8	0.26	14	0.5	0.7	0.25	08	0.46	0.97	0.32	14

Note: δ (mm/s) = isomer shift with respect to that of a α-Fe foil, ΔE_Q (mm/s) = quadrupole splitting, Γ (mm/s) = full width at half maximum, *RA* (%) = relative area of components. The error on the determination of the Mössbauer spectral parameters was estimated at ±0.02 mm/s by analyzing three samples of each product.

mm/s.

Synthetic Fe^{2+}-Fe^{3+} green rusts (e.g., carbonate, chloride, oxalate, see Drissi et al. 1995; Refait and Génin 1997; Refait et al. 1998c) give rise to two Fe^{2+} quadrupole doublets. The abundance of the additional doublet D_2 depends on the nature of the intercalated anions and, for example, is larger in $GR(C_2O_4^{2-})$ than in $GR(CO_3^{2-})$. The limit is $GR(SO_4^{2-})$ where D_2 is not observed (Cuttler et al. 1990; Refait et al. 1999). For this reason, D_2 was interpreted to be due to the influence of the anions of the interlayers upon the Fe^{2+} atoms of the hydroxide sheets. The presence of doublet D_2 in the spectrum of the GR mineral then excludes the possibility that SO_4^{2-} is the intercalated anion.

The existence of a second Fe^{3+} doublet D_4 is unusual. Such a doublet does not appear on the spectra of Fe^{2+}-Fe^{3+} hydroxysalts. For this reason, it can be attributed to the presence of Mg^{2+} ions as next nearest neighbors. Consistently, the intensity of D_4 increases with the Mg content, 8 vs. 14% for $Fe_4^{2+}Mg_2^{2+}Fe^{3+}{}_2\,(OH)_{16}\,CO_3$ vs. $Fe_2^{2+}Mg_2^{2+}Fe_2^{3+}\,(OH)_{12}\,CO_3$. As is seen in Figure 8c, doublet D_4 proved also necessary to fit the spectrum of the mineral. Its abundance, computed at 14%, is similar to those found for the synthetic hydroxycarbonates, and

more precisely matches that of $Fe^{2+}_2Mg^{2+}_2Fe^{3+}_2(OH)_{12}CO_3$.

The line widths observed on the three spectra are relatively small, and similar to what is usually observed for GRs without Mg^{2+} cations at the same temperature (Drissi et al. 1995; Refait et al. 1997; Koch 1998). These features are rather typical of well-defined cation positions and ordered arrangements (Koch 1998), confirming that each trivalent cation is more likely surrounded in each case by six divalent cations (Vucelic et al. 1997).

DISCUSSION

The GR mineral "fougerite" is difficult to analyze because it is (1) diluted in the soil, with a Fe content of 2–3.9% Fe_2O_3 according to Trolard et al. (1996) and (2) very reactive with respect to oxygen. Therefore, chemical analyses of the whole soil could be performed, but not those of the mineral alone. Similarly, XRD analyses of the soil failed to provide information. That is the reason why it was necessary to use techniques that are only sensitive to the GR mineral, namely ^{57}Fe Mössbauer spectroscopy and X-ray absorption spectroscopy at the Fe *K* edge.

The results obtained from both XAS and TMS spectroscopy suggest that Mg^{2+} substitutes for Fe^{2+}. The presence of Mg in the mineral is not surprising. First, the effective ionic radii of Mg^{2+} and Fe^{2+} ions in six-coordination are similar: 0.072 nm for Mg^{2+}, and 0.078 nm for high spin Fe^{2+} according to Shannon (1976), and many minerals, such as olivines, pyroxenes, amphiboles, and micas possess such a complete solid solution. Second, Mg is largely present in soils derived from weathering of granite, and especially of granodiorite as is the case in Fougères. The average MgO content in the unweathered rock is about 2% in the Fougères granodiorite with cordierite (BRGM 1981). The gley soil studied here is directly derived from a granodioritic area, with weatherable minerals, such as biotite present at shallow depth. In the spring water nearby the site studied here, Mg concentrations are ~10^{-4} *M*, much larger than Ca concentration (~$6\cdot10^{-5}$ *M*), whereas Al concentration is very low (~$4\cdot10^{-6}$*M*). These two factors largely favor substitution of Fe^{2+} by Mg^{2+} with respect to any other cation, though minor substitutions cannot be definitively ruled out.

The chemical formula of the GR mineral can then be more completely written as $[Fe^{2+}_{(1-x)}Mg^{2+}_yFe^{3+}_x(OH)_{2+2y}]^{+x}\cdot[x/n\ A^{n-}\cdot(1-x+y)\ H_2O]^{-x}$, where A^{n-} is the intercalated anion, and where one water molecule is supposedly intercalated over each Mg-occupied site as for Fe^{+2}. The quantities of Mg^{2+} which are incorporated cannot be determined precisely.

The presence of Mg^{2+} moreover would explain the variability of the Fe^{2+}/Fe^{3+} ratio that was observed in the GR mineral (Génin et al. 1998). According to various studies, most of the synthetic GR compounds exhibit a well defined composition with a specific Fe^{2+}/Fe^{3+} ratio. This is the case for $GR(CO_3^{2-})$ and $GR(SO_4^{2-})$ with a ratio of 2 (Hansen 1989; Drissi et al. 1995; Cuttler et al. 1990; Refait et al. 1999) and $GR(C_2O_4^{2-})$ with a ratio of 3 (Refait et al. 1998c). The exception is $GR(Cl^-)$ which is characterised by a variable ratio (Refait et al. 1998b). These variations, however are still approximately in the range between 2 and 3. Similar trends are observed for most of the pyroaurite-like compounds independently of the nature of the divalent and trivalent cations. This is generally interpreted in terms of cation ordering (Gastuche et al. 1967; Taylor 1969, 1973; Allmann 1970; Brindley and Kikkawa 1979): if trivalent cations M^{3+} never occupy neighboring sites, then the maximum M^{3+} content would correspond to a limit over which this ordering would not be possible, and this limit is $M^{2+}/M^{3+} = 2$. In contrast, the composition of the GR mineral proved to have important variability, with a Fe^{2+}/Fe^{3+} ratio able to vary from 2 to 1/2. The presence of another divalent cation along with Fe^{2+} in the brucite-like sheets would explain how the Fe^{2+}/Fe^{3+} ratio, which is now dissociated from the divalent/trivalent ratio, can be smaller than 2. The constraint on M^{2+}/M^{3+} can be then expressed as: $(1-x+y)/x \geq 2$, or equivalently $y \geq 3x - 1$.

Assuming for example a M^{2+}/M^{3+} ratio equal to 3 as in pyroaurite $Mg_6Fe_2(OH)_{16}CO_3\cdot4H_2O$, the chemical compositions of the mineral could be, according to the Fe^{2+}/Fe^{3+} ratios observed in the field (Génin et al. 1998):

If $Fe^{2+}/Fe^{3+} = 2$, $[Fe^{2+}_2MgFe^{3+}(OH)_8]^+\ [1/n\ A^{n-}\cdot m\ H_2O]^-$ and Mg/Fe = 1/3;

If $Fe^{2+}/Fe^{3+} = 1$, $[Fe^{2+}Mg_2Fe^{3+}(OH)_8]^+\ [1/n\ A^{n-}\cdot m\ H_2O]^-$ and Mg/Fe = 1;

If $Fe^{2+}/Fe^{3+} = 1/2$, $[Fe^{2+}Mg_5Fe^{3+}_2(OH)_{16}]^{2+}\ [2/n\ A^{n-}\cdot m\ H_2O]^{2-}$ and Mg/Fe = 5/3.

Larger Mg substitutions are of course possible depending on the abundance of Mg in the soil environment. The variability of the Fe^{2+}/Fe^{3+} ratio for the GR mineral can thus have two origins: variations of the Mg content on the one hand, variations on the overall divalent/trivalent ratio on the other hand. As demonstrated by the powder-XRD and TMS analyses of the synthetic Mg^{2+}-Fe^{2+}-Fe^{3+} hydroxycarbonates, this M^{2+}/M^{3+} ratio can indeed vary, more likely in the range of 2 to 3 as in other similar minerals. A geochemical implication is that as oxidation proceeds, more Mg is incorporated in the structure.

There remain two major unknown factors: (1) the nature of the interlayer anions, which cannot be directly derived from EXAFS or Mössbauer data and, (2) the stability and the reactivity of the solid solution intermediate compounds between GRs and Mg^{2+}-Fe^{3+} pyroaurite-like hydroxysalts.

ACKNOWLEDGMENTS

The authors thank V. Briois and R. Revel at LURE for assistance with XAS experiments and F. Bouamrane for the preparation of the samples. Supports from Institute National de la Recherche Agronomiyve, the Region Brehagne, and the French National Program on Soil and Erosion (P.N.S.E.) are gratefully acknowledged.

REFERENCES CITED

Allmann, R. (1968) The crystal structure of pyroaurite. Acta Crystallographica, B24, 972–977.

———(1970) Doppelschichtstrukturen mit brucitähnlichen Schichtionen $[Me(II)_{1-x}Me(III)_x(OH)_2]^{x+}$. Chimia, 24, 99–108.

Arden, T.V. (1950) The solubility products of ferrous and ferrosic hydroxides. Journal of the Chemical Society, 24, 882–885.

Bianconi, A. (1980) Surface X-ray absorption spectroscopy: surface EXAFS and surface XANES. Applied Surface Science, 6, 392–418.

Bourrié, G., Trolard, F., Génin, J.-M. R., Jaffrezic, A., Maître, V., and Abdelmoula, M. (1999) Iron control by equilibria between hydroxy-green rusts and solutions in hydromorphic soils. Geochimica et Cosmochimica Acta, 63, 3417–3427.

BRGM (1981) Carte géologique de la France à 1/50 000. Fougères 13–17. Service Géologique National, Orléans.

Brindley, G.W. and Kikkawa, S. (1979) A crystal-chemical study of Mg, Al and Ni, Al hydroxy-perchlorates and hydroxy-carbonates. American Mineralogist, 64, 836–843.

Citrin, P.H. (1986) An overview of SEXAFS during the past decade. Journal de Physique, 47–C8, 438–472.

Cuttler, A.H., Man, V., Cranshaw, T.E., and Longworth, G. (1990) A Mössbauer study of green rust precipitates: I. Preparations from sulphate solutions. Clay Minerals, 25, 289–301.

Drissi, S.H., Refait, Ph., and Génin, J.-M.R. (1994) The oxidation of $Fe(OH)_2$ in the presence of carbonate ions: Structure of carbonate green rust one. Hyperfine Interactions, 90, 395–400.

Drissi, S.H., Refait, Ph., Abdelmoula, M., and Génin, J.-M.R. (1995) Preparation and thermodynamic properties of Fe(II)-Fe(III) hydroxide-carbonate (green rust one), Pourbaix diagram of iron in carbonate-containing aqueous media. Corrosion Science, 37, 2025–2041.

Ferrier, A. (1966) Influence de l'état de division de la goethite et de l'oxyde ferrique sur leur chaleur de réaction. Revue de Chimie Minérale, 3, 587–615.

Garrels, R.M. and Christ, C.L. (1965) Solutions, minerals and equilibria. Harper and Row.

Gastuche, M.C., Brown, G., and Mortland, M.M. (1967) Mixed magnesium-aluminium hydroxides. Clay Minerals, 7, 177–192.

Génin, J.-M.R., Bourrié, G., Trolard, F., Abdelmoula, M., Jaffrezic, A., Refait, Ph., Maître, V., Humbert, B., and Herbillon, A. (1998) Thermodynamic equilibria in aqueous suspensions of synthetic and natural Fe(II)-Fe(III) green rusts: occurrences of the mineral in hydromorphic soils. Environmental Science and Technology, 32, 1058–1068.

Génin, J.-M.R., Refait, Ph., Bourrié, G., Abdelmoula, M., and Trolard, F. (2001) Structure and stability of Fe(II)-Fe(III) green rust mineral and its potentiality for reducing pollutants in soil solutions. Applied Geochemistry, 16, 559–570.

Hansen, H.C.B. (1989) Composition, stabilization, and light absorption of Fe(II)-Fe(III) hydroxide-sulphate (green rust) and its reduction of nitrite. Clay Minerals, 24, 663–669.

Hansen, H.C.B., Koch, C.B., Nancke-Krogh, H., Borggaard, O. K., and Sørensen, J. (1996) Abiotic nitrate reduction to ammonium: key role of green rust. Environmental Science and Technology, 30, 2053–2056.

Huber, N.K. and Garrels, R.M. (1953) Relation of pH and oxidation potential to sedimentary iron mineral formation. Economic Geology, 48, 337–357.

Koch, C.B. (1998) Structures and properties of anionic clay minerals. Hyperfine Interactions, 117, 131–157.

Krumbein, W.C. and Garrels, R.M. (1952) Origin and classification of chemical sediments in terms of pH and oxidation-reduction potentials. Journal of Geology, 60, 1–33.

Kuzmin, A. and Parent, P. (1994) Focusing and superfocusing effects in X-ray absorption fine structure at the iron K edge in FeF_3. Journal of Physics, Condensed Matter, 6, 4395–4404.

Lee, P.A. and Pendry, J.B. (1975) Theory of the EXAFS. Physical Review B, 11, 2795–2811.

Lindsay, W. L. (1979) Chemical equilibria in soils. Wiley Interscience, New York.

Loyaux-Lawniczak, S., Refait, Ph., Lecomte, P., Ehrhardt, J.-J., and Génin, J.-M.R. (1999) The reduction of chromate ions by Fe(II) layered hydroxides. Hydrology and Earth System Sciences, 3, 593–599.

Loyaux-Lawniczak, S., Refait, Ph., Ehrhardt, J.-J., Lecomte, P., and Génin, J.-M.R. (2000) Trapping of Cr by formation of ferrihydrite during the reduction of chromate ions by Fe(II)-Fe(III) hydroxysalt green rusts. Environmental Science and Technology, 34, 438–443.

Mendiboure, A. and Schöllhorn, R. (1986) Formation and anion exchange reactions of layered transition metal hydroxides $[Ni_{1-x}M_x](OH)_2(CO_3)_{x/2}(H_2O)_z$ (M=Fe,Co). Revue de Chimie Minérale, 23, 819–827.

Miyata, S. (1983) Anion-exchange properties of hydrotalcite-like compounds. Clays and Clay Minerals, 31, 305–311.

Myneni, S.C.B., Tokunaga, T.K., and Brown, G.E. Jr. (1997) Abiotic selenium redox transformations in the presence of Fe(II,III) oxides. Science, 278, 1106–1109.

Ponnamperuma, F.N. (1972) The chemistry of submerged soils. Advance in Agronomy, 24, 173–189.

Ponnamperuma, F.N., Tianco, E.M., and Loy, T. (1967) Redox equilibria in flooded soils: I. the iron hydroxide system. Soil Science, 103, 374–381.

Refait, Ph. and Génin, J.-M.R. (1997) Mechanisms of oxidation of Ni(II)-Fe(II) hydroxides in chloride-containing aqueous media: role of the pyroaurite-type Ni-Fe hydroxychlorides. Clay Minerals, 32, 597–613.

Refait, Ph., Drissi, S.H., Pytkiewicz, J., and Génin, J.-M.R. (1997) The anionic species competition in iron aqueous corrosion: role of various green rust compounds. Corrosion Science, 39, 1699–1710.

Refait, Ph., Abdelmoula, M., and Génin, J.-M.R. (1998a) Oxidation of pyroaurite-like Ni-Fe hydroxychlorides studied by Mössbauer spectroscopy at 16 K. Clay Minerals, 33, 665–669.

———(1998b) Mechanisms of formation and structure of green rust one in aqueous corrosion of iron in the presence of chloride ions. Corrosion Science, 40, 1547–1560.

Refait, Ph., Charton, A., and Génin, J.-M.R. (1998c) Identification, composition, thermodynamic and structural properties of a pyroaurite-like Fe(II)-Fe(III) hydroxyoxalate green rust. European Journal of Solid State and Inorganic Chemistry, 35, 655–666.

Refait, Ph., Drissi, S.H., Simon, L., and Génin, J.-M.R. (1998d) Mössbauer analysis of pyroaurite-type Mg(II)-Fe(III) hydroxy-salt green rust compounds. Hyperfine Interactions, C3, 372–375.

Refait, Ph., Bon, C., Simon, L., Bourrié, G., Trolard, F., Bessière, J., and Génin, J.-M. R. (1999) Chemical composition and Gibbs standard free energy of formation of Fe(II)-Fe(III) hydroxysulphate green rust and Fe(II) hydroxide. Clay Minerals, 34, 499–510.

Refait, Ph., Simon, L., and Génin, J.-M.R. (2000) Reduction of SeO_4^{2-} anions and anoxic formation of iron(II)-iron(III) hydroxy-selenate Green Rust. Environmental Science and Technology, 34, 819–825.

Ressler, T. (1997) WinXAS: A new software package not only for the analysis of energy-dispersive XAS data. Journal de Physique, IV, 7, C2–269.

Roussel, H., Briois, V., Elkaim, E., de Roy, A., and Besse, J.P. (2000) Cationic order and structure of [Zn-Cr-Cl] and [Cu-Cr-Cl] layered double hydroxides: a XRD and EXAFS study. Journal of Physical Chemistry, B25, 5915–5953.

Shannon, R.D. (1976) Revised effective ionic radii and systematic studies of interatomic distances in halides and chalcogenides. Acta Crystallographica, A32, 751–767.

Sillén, L.G. (1967) Master variables and activity scales. In Equilibrium concepts in natural water systems, Ed., W. Stumm, Advance In Chemistry Series 67, p. 47–56. American Chemical Society, Washington, D.C.

Stohr, J. (1986) In R. Prins and D. Koningsberger, Eds., X-ray absorption: Principles, Applications, Techniques of EXAFS, SEXAFS and XANES, p. 443. Wiley, New York.

Tadjeddine, A. (1994) In situ X-ray absorption spectroscopy investigation of UPD metal monolayers. In C.A. Melendres and A. Tadjeddine, Eds., Synchrotron Techniques in Interfacial Electrochemistry, p. 215–245. Kluwer, Dordrecht, Boston, London.

Taylor, H.F.W. (1969) Segregation and cation ordering in sjögrenite and pyroaurite. Mineralogical Magazine, 37, 338–342.

———(1973) Crystal structures of some double hydroxide minerals. Mineralogical Magazine, 39, 377–389.

Taylor, R.M. (1981) Color in soils and sediments—A review. In H. Van Olphen and F. Veniale, Eds., International Clay Conference 1981, Developments in Sedimentology, 35, p. 749–761. Elsevier, New York.

Teo, B.K. (1986) EXAFS: Basic principles and data analysis, vol. 9. Springer Verlag, Berlin

Trolard, F. and Tardy, Y. (1987) The stabilities of gibbsite, boehmite, aluminous hematites in bauxites, ferricretes and laterites as a function of water activity, temperature and particle size. Geochimica et Cosmochimica Acta, 51, 945–957.

Trolard, F., Abdelmoula, M., Bourrié, G., Humbert, B., and Génin, J.-M.R. (1996) Evidence of the occurrence of a "Green Rust" component in hydromorphic soils—Proposition of the existence of a new mineral: "fougérite". Comptes Rendus de l'Académie des Sciences, 323 Série IIA, 1015–1022.

Trolard, F., Génin, J.-M.R., Abdelmoula, M., Bourrié, G., Humbert, B., and Herbillon, A.J. (1997) Identification of a greeen rust mineral in a reductomorphic soil by Mössbauer and Raman spectroscopies. Geochimica et Cosmochimica Acta, 61, 1107–1111.

Vucelic, M., Jones, W., and Moggridge, G.D. (1997) Cation ordering in synthetic layered double hydroxides. Clays and Clay Minerals, 45, 803–813.

Vysotskii, G.N. (1905) Gley. Pochvovedenie, 4, 291–327 (original paper in Russian).

———(1999) Gley. An abridged publication of Vysotskii 1905 on the 257th Anniversary of the Russian Academy of Sciences. Eurasian Soil Science, 32, 1063–1068.

MANUSCRIPT RECEIVED JULY 10, 2000
MANUSCRIPT ACCEPTED JANUARY 26, 2001
MANUSCRIPT HANDLED BY MICHAEL E. FLEET